First-principles study of cubic Bi pyrochlores

Beverly Brooks Hinojosa,[1] Juan C. Nino,[2] and Aravind Asthagiri[1,*]
[1]*Department of Chemical Engineering, University of Florida, Gainesville, Florida 32611, USA*
[2]*Department of Materials Science and Engineering, University of Florida, Gainesville, Florida 32611, USA*
(Received 6 November 2007; revised manuscript received 25 February 2008; published 31 March 2008)

We examined a range of cubic $Bi_2B_2O_6O'$ (B=Ti, Ru, Rh, Ir, Os, and Pt) pyrochlores with density functional theory (DFT) calculations and report the structural parameters along with the electronic structure of the bismuth pyrochlores in their ideal cubic, defect-free structure. We also examined the role of cation displacements within the cubic structure and find that only $Bi_2Ti_2O_7$ shows a substantial increase in favorability with Bi cation displacements. For $Bi_2Ti_2O_7$, we find an average displacement of 0.38 ± 0.02 Å for the Bi cation and an energy change of 0.146 ± 0.001 eV/Bi atom. The cation displacement in $Bi_2Ti_2O_7$ follows the spin-ice rules reported in complex Bi-based pyrochlores, where two-long and two-short bonds are found in each tetrahedron of Bi_4O'. Examination of the electronic structure shows the main driving force in the displacement is the extent of Bi-O' interactions in $Bi_2Ti_2O_7$ and metallic bismuth pyrochlores. In $Bi_2Ti_2O_7$, we observe more overlap of Bi s and p states with O $2p$ states, similar to the reported electronic structure of $Bi_2Sn_2O_7$, PbO, and SnO, which leads to the asymmetric electronic structure around the Bi cation. This asymmetric electron structure is associated with the displacement of cations in $Bi_2Ti_2O_7$. Our DFT results match the general understanding from experimental studies but underestimate the displacement in $Bi_2Ru_2O_7$.

DOI: 10.1103/PhysRevB.77.104123 PACS number(s): 71.20.−b, 78.55.Hx, 71.15.Pd

I. INTRODUCTION

Pyrochlore oxides have received much attention for several decades due to their diverse physical properties, which allow for a broad range of applications, such as high-permittivity dielectrics,[1] solid electrolytes,[2] host materials for the immobilization of fission products,[3,4] catalysis,[5] and thermal barrier coatings.[6–8] Ideal stoichiometric pyrochlores ($A_2B_2O_7$) are cubic with space group $Fd\bar{3}m$ and often described as two interpenetrating networks of B_2O_6 octahedra and A_2O' tetrahedra,[9,10] as shown in Fig. 1. The overall formula is typically represented as $A_2B_2O_6O'$ to distinguish the oxygen within the two networks. Figure 1 represents one of a multitude of perspectives of the pyrochlore structure found in the literature (see Refs. 10–14 for more extensive discussion on pyrochlore structure). From extensive experimental work on the synthesis and structural characterization of cubic pyrochlores, stability fields have been proposed for allowable substitution into the A and B cation sites based on simple measures such as the ratio of the cation radii size and the cation electronegativity.[9,12] The typical A (B) cation radii is around 1 (0.6) Å, but compounds with variations of up to 0.2 Å for both cations are stabilized. As the cation radii shift away from the typical values noted, the range of A/B substitutions that stabilize into a stoichiometric cubic structure sharply decreases.[9] Recent experimental work extended the stability field of allowable cation radius ratios with structures that incorporate large static atomic displacements and macroscopically retain the cubic symmetry.[15–17] For an excellent but somewhat dated survey of known cubic pyrochlores, see Ref. 9.

Recent attention has focused on bismuth based pyrochlores, where the Bi^{3+} cation resides in the A site for their potential use in capacitor and high-frequency filter applications.[13,14,18] Bismuth has a lone pair of electrons and the cation radius is 1.17 Å,[19] making it one of the larger A cations found in the pyrochlore family and results in a relatively small region of stability in the structure field maps.[9] In the past decade, experimental work extended this stability region, with the synthesis of numerous complex Bi pyrochlores that incorporate substitutions of small cations in both the A and B sites. The most extensively studied of these materials is $Bi_{3/2}Zn_{0.92}Nb_{3/2}O_{6.92}$ (BZN).[1,10,13,20–25] Structure and spectroscopic probes reveal a large amount of displacive disorder on both the A and O' ions that led Withers *et al.*[10] to propose several ordering principles on the A_2O' network for these materials based on x-ray diffraction studies. The large displacements of the ions in BZN and other complex bismuth-based pyrochlores, such as $Bi_{3/2}ZnTa_{3/2}O_7$, $Bi_{3/2}MgNb_{3/2}O_7$, and $Bi_{3/2}MgTa_{3/2}O_7$, are critical to the observed high dielectric permittivity.[26] There is still a need to better understand the nature of the cation displacements. Interestingly, some of the more simple bismuth pyrochlores (i.e., without cation substitution) are reported to have cation displacements. In particular, large cation displacements are reported for $Bi_2Ru_2O_7$ (Ref. 15) and $Bi_2Ti_2O_7$ in both the stoichiometric[16] and defective form.[17] The simple bismuth pyrochlores are of interest from a technological viewpoint[27–29] and also allow for examining the role of cation displacements without the influence of substitutions on the cation sites.

The majority of the work on A-site bismuth pyrochlores are experimental with only a few recent density functional theory (DFT) studies of $Bi_2Sn_2O_7$,[30] $Bi_2Ti_2O_7$,[14] and $Bi_2Ru_2O_7$.[15] The DFT work on bismuth pyrochlores are restricted to its ideal cubic structure, except for the work of Walsh *et al.*[30] which examined the low temperature, monoclinic phase of $Bi_2Sn_2O_7$. DFT can be an invaluable tool in systematically exploring and providing insight into the role of structure, composition, and atomic relaxation on the properties of pyrochlores. While the experimental work provided details of the structure of several bismuth pyrochlores, synthesis of these materials is nontrivial and often results in O deficiencies. The density and nature of these O deficiencies can vary and sometimes were not identified in early experi-

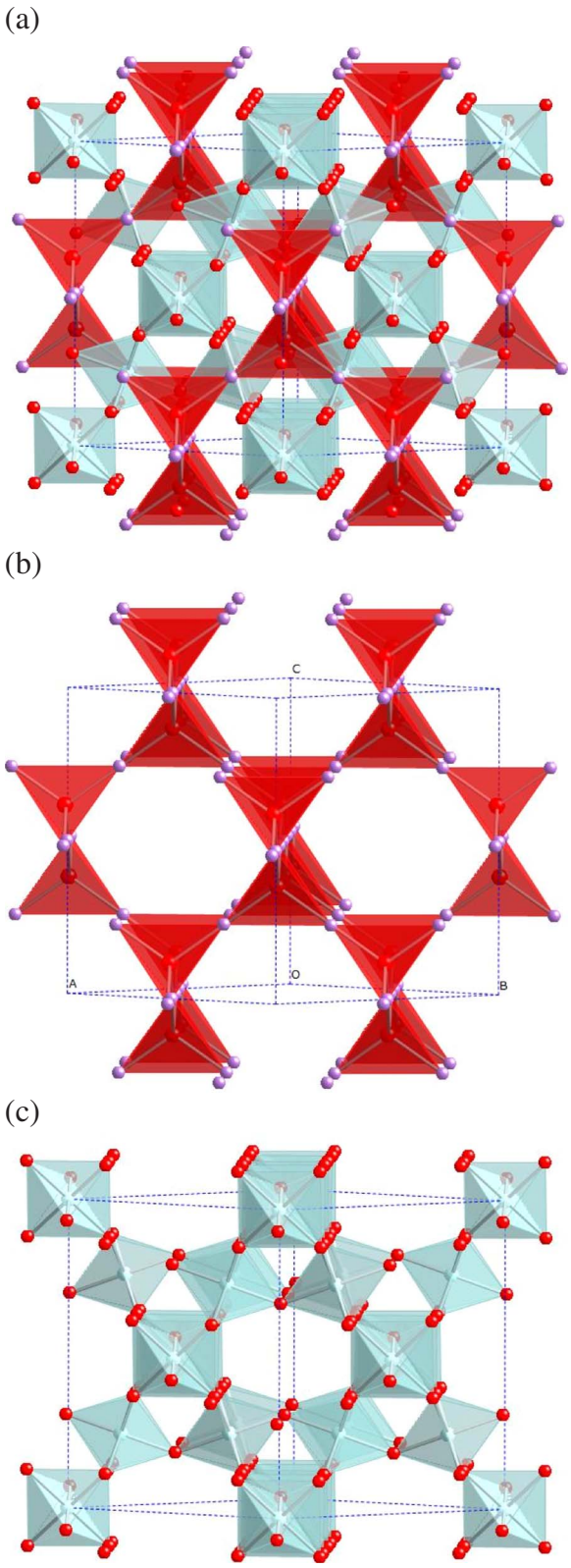

FIG. 1. (Color online) The (a) ideal $A_2B_2O_6O'$ pyrochlore structure and the two interpenetrating subnetworks: (b) A_2O' tetrahedrons and (c) B_2O_6 octahedrons.

mental work. The presence of O deficiencies introduces additional complexities since their influence on deviations from the cubic pyrochlores is not well understood. Comparisons between experiment and DFT calculations of ideal defect-free pyrochlores will allow us to identify deviations due to the presence of deficiencies. DFT can also help us to establish connections between the electronic structure and the observed structural behavior in the Bi pyrochlores. Of particular interest is the role of the Bi lone pair in the experimentally reported large cation displacement in some bismuth pyrochlores.[14–17] The lone pair of Bi is believed to create stereochemical constriction, leading to more distorted structures that deviate from the ideal cubic form found in other families of pyrochlores. The reduction of this lone pair nature due to mixing of orbitals between the Bi and *B*-site cations is proposed to explain the lack of distorted structures in the bismuth metallic pyrochlores.[5,31,32] A systematic study of the differences in electronic structure of various bismuth pyrochlores, including insulating versus metallic, will be important in clarifying the role of the lone pair in bismuth pyrochlores. In this paper, we report DFT calculations on a range of simple cubic bismuth containing pyrochlores $Bi_2B_2O_6O'$ (B=Ti, Ru, Rh, Ir, Os, and Pt) that have been experimentally synthesized.[5,9,15–17,31] We initially examined the above bismuth pyrochlores within the ideal cubic pyrochlores structure. Subsequently, we investigated the potential role of cation displacements in stabilizing the cubic bismuth pyrochlores.

II. CALCULATION DETAILS

First-principles calculations were performed with Vienna *Ab initio* simulation package (VASP),[33–36] which is a plane-wave DFT code, using the projector augmented wave (PAW) pseudopotentials provided in the VASP database.[37,38] We include the Bi($5d$,$6s$,$6p$), O($2s$,$2p$), Rh($4p$,$4d$,$5s$) Ti($3s$,$3p$,$3d$,$4s$), Ru($4p$,$4d$,$5s$), Os($5p$,$5d$,$6s$), Ir($5d$,$6s$), and Pt($5d$,$6s$) orbitals as the valence electrons. The DFT calculations were performed within the local density approximation (LDA).[39] The LDA is expected to underestimate lattice constants and overestimate the strength of bonding but has been found to be more accurate than the gereralized gradient approximation (GGA) functionals for many metal oxides[40,41] and in a recent study of La and Y-based pyrochlores.[42] The GGA with the parametrization of Perdew *et al.*[43] was tested and provided qualitative agreement with the results reported in this paper. Electronic relaxation was performed with the conjugate gradient method accelerated using Methfessel–Paxton Fermi-level smearing with a Gaussian width of 0.1 eV.[44] The ideal $Fd\bar{3}m$ space group symmetry was tested and the bismuth pyrochlores examined in this work retain the ideal structure. Therefore, all calculations were performed at fixed volume and shape, while the atoms were relaxed until the forces were less than 0.001 eV/Å. A plane-wave cutoff energy of 400 eV was used along with a $6\times6\times6$ Monkhorst–Pack[45] mesh, resulting in ten irreducible k points. Test calculations done with 450 eV cutoff and a $8\times8\times8$ mesh result in differences less than 0.02 eV/88 atom cell in the total energy, well within the error for the results presented in this paper. We performed several test calculations to confirm that spin polarization

does not affect any of the results; therefore, all data reported in this paper are without spin polarization.

As mentioned before, ideal pyrochlores usually adopt the $Fd\bar{3}m$ space group, which has two possible origin choices at either the 8*a* site (origin choice 1) or the 16*c* site (origin choice 2).[46] Origin choice 2 is more commonly used in the literature and exclusively used within this work. Within origin choice 2, the ideal sites occupied are the 16*d* site (0.5,0.5,0.5), 16*c* site (0,0,0), O anion at the 48*f* site (x,0.125,0.125), and O′ anion at either the 8*a* site (0.125,0.125,0.125) or the 8*b* site (0.375,0.375,0.375). If the large *A* cation is in the 16*d* site (0.5,0.5,0.5), the configuration is termed *B* centered with the small *B* cation, occupying the 16*c* site (0,0,0) and the O′ anion at the 8*b* site (0.375,0.375,0.375). Alternatively, in the *A*-centered configuration, the *A* cation occupies the 16*c* site (0,0,0) with the *B* cation at the 16*d* site (0.5, 0.5, 0.5) and the O′ anion at the 8*a* site (0.125,0.125,0.125). Unless otherwise noted, the *B*-centered configuration is used in this paper and, where needed, experimental results are converted to this configuration for comparison. By symmetry, only the O 48*f* atoms can relax in the ideal cubic pyrochlores, and therefore, the entire structure is explained by two parameters: the cubic lattice constant and the oxygen positional parameter (x). The value of x depends on the occupant of the 16*c* site (0,0,0) and the relationship between the *A*- and *B*-centered configurations is $x(A)=0.75-x(B)$.[46] There are known bounds observed in the value of x based on the oxygen polyhedral coordination at the 48*f* site surrounding the *A* and *B* cations. If the oxygen ions form a regular octahedral (cube), the resulting value for $x(B)$ would be 0.3125 (0.375). We also examined the role of displacing the cations and O′ atoms from their high symmetry positions and the details of these calculations are presented in Sec. III B.

III. RESULTS AND DISCUSSION

A. Ideal bismuth pyrochlores

For each of the bismuth pyrochlores ($Bi_2B_2O_6O'$, *B*=Ti, Ru, Rh, Ir, Os, and Pt), we determine the equilibrium lattice parameter by generating energy versus volume curves. These relaxed structures retain the ideal pyrochlore structure as discussed in Sec. II. The key structural parameters (lattice parameter and oxygen positional parameter) for the relaxed structures of all the simple pyrochlores examined are reported, along with experimental data as a function of *B* cation radius in Figs. 2 and 3 and in Table I. The *B* cation radii, taken from Ref. 19, were useful in defining stability field maps for simple pyrochlores.[9] In several families of pyrochlores, the *B* cation radii were shown to correlate with structural, mechanical, and thermal properties when examined using empirical potentials.[4,8,47,48] Figure 2(a) shows that our DFT results for the lattice constants are within ~1% of the experimental values. By considering that LDA underestimates lattice constants, this level of accuracy is excellent and on par with previous DFT studies.[42] The lattice parameter of the $Bi_2Ti_2O_7$ system shows the largest deviation and is underestimated by 1.2%. For the oxygen positional parameter, as shown in Fig. 2(b), the results are within ~0.5% of the experimental data except for $Bi_2Ti_2O_7$, which shows an error of nearly 2% overestimation. $Bi_2Ti_2O_7$ falls outside the stability field predicted based on the ratio of cation radius but was recently synthesized with and without O′ defects.[16,17] Diffraction studies showed that bismuth and the O′ atoms displace in the $Bi_2Ti_2O_7$ pyrochlore.[16,17] We attribute the differences in the structural parameters between our DFT calculations and experimental results for $Bi_2Ti_2O_7$ to the Bi cation displacement. A recent study of defective $Bi_2Ru_2O_7$ (Ref. 15) also reported Bi displacements with small displacement of the oxygen in the 8*b* site. For $Bi_2Ru_2O_7$, we do not find a large deviation for either the lattice parameter or the x positional parameter between our DFT results with no cation

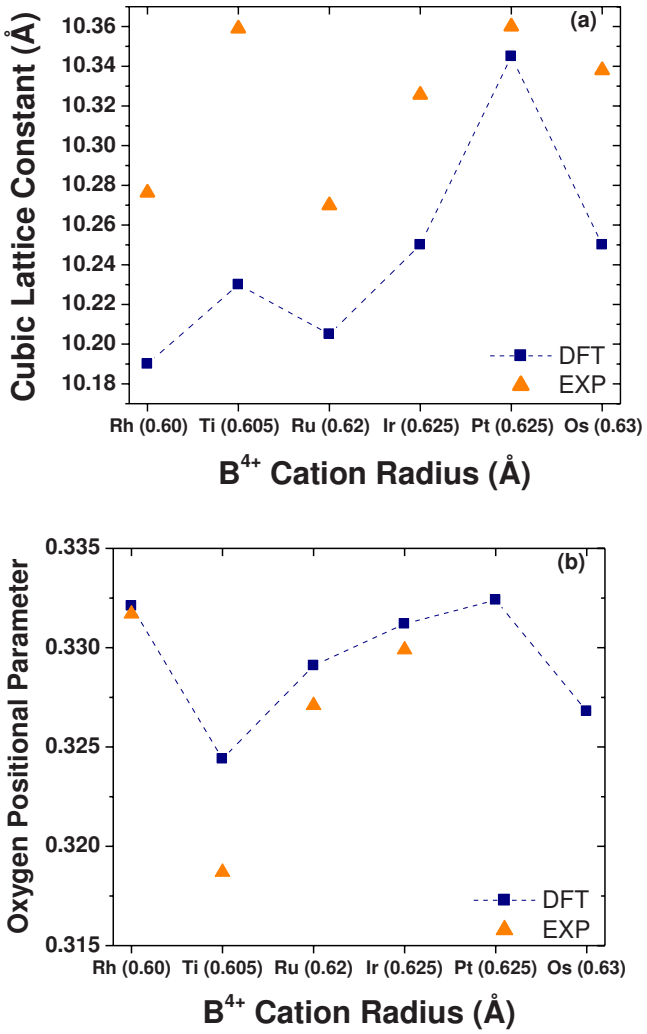

FIG. 2. (Color online) The dependence of the (a) cubic lattice constant and (b) the oxygen positional parameter on the B^{4+} cation radius as determined by DFT (square) and experiment (triangle) for Rh, (Ref. 31) Ti, (Refs. 16 and 17) Ru, (Ref. 15) Ir, (Ref. 5) Pt, (Ref. 9) and Os (Ref. 9). The *A*-centered configuration oxygen positional parameter values reported for $Bi_2Ti_2O_7$ (Refs. [16,17]) are converted to the *B*-centered configuration value (see Sec. II for discussion on *A*- versus *B*-centered configuration). The dashed lines drawn between our DFT values included as a visual aid. Note that Ir and Pt have the same ionic radius of 0.625 Å.

TABLE I. The cubic lattice constant (a), oxygen positional parameter (x), Bi-O′ ($d_{(\text{A-O}')}$) length, Bi-O 48f ($d_{(\text{A-O }48f)}$) length, B-O 48f ($d_{(B\text{-O }48f)}$) length, and B-O-B angle in order of cation radius for $Bi_2Rh_2O_7$, $Bi_2Ti_2O_7$, $Bi_2Ru_2O_7$, $Bi_2Ir_2O_7$, $Bi_2Pt_2O_7$, and $Bi_2Os_2O_7$. Italicized values represent the average values, while + and * denote experimental studies conducted at room temperature and low temperature ($\leqslant$12 K), respectively.

	a (Å)	x (Å/Å)	$d_{(\text{A-O}')}$ (Å)	$d_{(\text{A-O }48f)}$ (Å)	$d_{(B\text{-O }48f)}$ (Å)	B-O-B (deg)
		$Bi_2Rh_2O_7$				
This Work	10.190	0.332	2.206	2.485	1.986	130.2
Experimental $Bi_{1.95}Rh_2O_{6.83}$+,[a]	10.2764	0.3317	2.2249	2.508	2.001	
		$Bi_2Ti_2O_7$				
This Work	10.230	0.3244	2.213	2.547	1.96	134
Experimental $Bi_2Ti_2O_7$*,[b]	10.359	0.3187	*2.289*	*2.559*	1.964	137.5
Experimental $Bi_{1.74}Ti_2O_{6.62}$+,[c]	10.3569	0.3187	2.277	*2.637*	1.9655	
		$Bi_2Ru_2O_7$				
This Work	10.205	0.3291	2.209	2.509	1.977	131.8
Experimental $Bi_{1.87}Ru_2O_{6.903}$*,[d]	10.2699	0.3271	*2.23*	*2.55*	1.98	
		$Bi_2Ir_2O_7$				
This Work	10.250	0.3312	2.219	2.505	1.994	130.6
Experimental $Bi_{1.9}Ir_2O_{6.8}$+,[e]	10.3256	0.3299	2.236	2.534	2.003	131.4
		$Bi_2Pt_2O_7$				
This Work	10.345	0.3324	2.239	2.519	2.018	129.9
Experimental $Bi_2Pt_2O_7$[f]	10.36					
		$Bi_2Os_2O_7$				
This Work	10.250	0.3268	2.219	2.536	1.976	133
Experimental $Bi_2Os_2O_7$[f]	10.338					

[a]Reference 31.
[b]Reference 16.
[c]Reference 17.
[d]Reference 15.
[e]Reference 5.
[f]Reference 9.

displacements and the experimentally reported structure with cation displacements.[15] We examine the role of Bi cation displacement in the bismuth pyrochlores in Sec. III B.

Excluding $Bi_2Ti_2O_7$, our DFT results for both lattice parameter and oxygen displacement parameter do not show any systematic correlation to B cation radii. It is important to stress that the DFT results follow the same trends as the experimental data. Barker *et al.*[49] found that x increases with increasing B^{4+} cation radius for various pyrochlores. As shown in Fig. 2(a), this simple relationship does not hold over the entire range of bismuth pyrochlores since the oxygen positional parameters for Rh and Os have an inverse relationship with respect to the B cation radii. A relationship between the B cation radii and cubic lattice constant has not been explicitly noted in the literature, but Minervini *et al.*[47] observed a strong linear relationship between lattice parameter and A cation radii for several families of B cation pyrochlores. A similar trend observed for some of the bismuth pyrochlores [see Fig. 2(a)] has some clear contradictions. Ir and Pt have the same cation radii but different lattice constants and the Os system has exactly the same lattice constant as Ir despite the larger cation radii. We attempted to plot the structural parameters with electronegativity and other definitions of the cation radius with no simple trends observed, indicating that the bonding in the bismuth based pyrochlores may be more complex than other pyrochlore families. As will be shown in Sec. III C, when we examine the electronic structure of these pyrochlores, there is a large degree of B cation dependent covalency in the bismuth pyrochlores. The lack of a relationship between structure and cation radii can be attributed to the covalent interactions and a similar observation was made in a recent DFT study of lanthanum and yttrium based pyrochlores involving the polarizable Sn cation.[42] It is worthwhile to note that the lattice constant for $Bi_2Ti_2O_7$ falls in a similar region to the other bismuth pyrochlores with corresponding cation radii. Kennedy[31] noted the larger lattice constants associated with the insulator (Ti and Sn) versus metal (Rh, Ru, and Ir) bismuth pyrochlores. Our "ideal" DFT calculations (i.e., no cation displacements) indicate that the larger lattice constant of

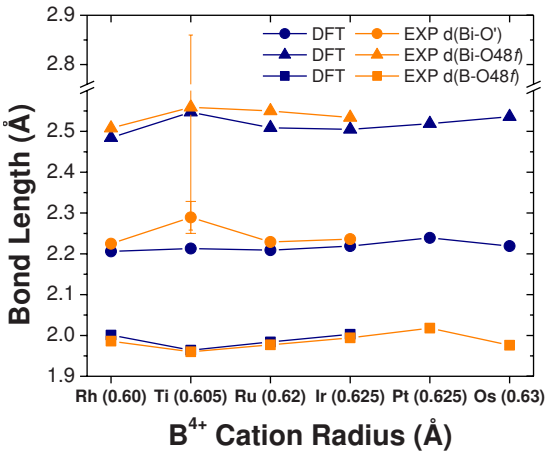

FIG. 3. (Color online) Bond lengths for Bi-O′, Bi-O 48*f*, and B-O 48*f* as a function of cation radius as determined by DFT (dark blue) and experiment (orange) for Rh, (Ref. 31) Ti, (Refs. 16 and 17) Ru, (Ref. 15) Ir, (Ref. 5) Pt, (Ref. 9) and Os (Ref. 9). The lines drawn between the values included as a visual aid. Note that Ir and Pt have the same ionic radius of 0.625 Å.

the insulating bismuth pyrochlores (Ti and Sn) is related to the inclusion of cation displacements within these structures. As we will discuss in the next section, the inclusion of atomic displacement dramatically changes the lattice constant of $Bi_2Ti_2O_7$.

The relevant bond lengths for the pyrochlore structure from DFT and experiment are presented in Fig. 3. Overall, both Bi-O and Bi-O′ bond lengths compare well with experimental data, but as with the lattice constant and oxygen positional parameter, there is a larger difference in the $Bi_2Ti_2O_7$ system. For the $Bi_2Ti_2O_7$ system, the average experimental Bi-O 48*f* bond length compares very well, even with the exclusion of bismuth displacement. In the experimental study, the Bi-O′ bond length for $Bi_2Ti_2O_7$ is slightly larger than that observed in other bismuth pyrochlores. Since the Bi displacement is perpendicular to the O′-Bi-O′ chains, the Bi-O′ bond length lengthens by this displacement. The values for the bond lengths of *B*-O 48*f* compare well with experimental data for all the systems considered. Although not shown in Fig. 3, the bond angles in all six bismuth pyrochlores compare well to experimental values, but once again $Bi_2Ti_2O_7$ shows the largest deviation. Overall, the structural parameters shown in Figs. 2 and 3 compare well with the available experimental data, indicating that DFT accurately captures the structural relaxation in the simple bismuth pyrochlore systems, at least for systems without large cation displacements observed.

B. Bismuth pyrochlores with atomic displacement

To address the issue of the large deviations observed for $Bi_2Ti_2O_7$ relative to the other bismuth pyrochlores, we must examine the role of cation displacement. Experimentally, it is known that the bismuth ions displace from their ideal crystallographic site for some simple bismuth pyrochlores.[15–17] Due to the symmetry of our initial structure, the Bi atoms cannot displace during relaxation; only the O 48*f* atoms have nonzero forces at the initial structure. Therefore, it is possible that in all of our relaxations we are actually sitting on a saddle point with respect to displacements of the Bi atoms. Ideally, we would explore the phonon modes in the pyrochlore structure and identify any soft modes, but with the large unit cell, these calculations are computationally expensive. We used a simpler approach to investigate the role of bismuth displacement within these pyrochlores. For each Bi pyrochlores, we perform simulated annealing, beginning with the relaxed structures found in Sec. III A, with the volume fixed using *ab* initio molecular dynamics (MD).[33–36] This approach forces the Bi, *B* cations, and O′ ions out of their zero-force crystallographic sites. The simulated annealing consisted of MD simulations within the *NVT* ensemble starting at 1000 K and cooling to 300 K over 500 MD steps with a time step of 0.5 fs. While the simulated annealing procedure is over extremely short times, after 100 MD steps, the atoms displace from their high symmetry sites, indicating that the number of steps is sufficient to accomplish our primary goal. Due to the loss of symmetry within these displaced configurations, we perform the *ab initio* MD with only the Γ point. After simulated annealing, we minimize the system using the same approach outlined in Sec. II, except that have we used a $3\times3\times3$ *k* mesh (14 irreducible *k* points). Comparisons made in this section between displaced and undisplaced structures are from calculations using the $3\times3\times3$ mesh and we confirmed that the decrease in *k* mesh does not affect any of the conclusions.

Table II shows the energy change due to cation displacement and the average atomic displacements from the ideal positions of the $Fd\bar{3}m$ cubic pyrochlore structure for all the bismuth pyrochlores examined. Similar values for the atomic displacement reported from experimental studies of $Bi_2Ti_2O_7$ and $Bi_2Ru_2O_7$ are also included in Table II. In our calculations, only one system, i.e., $Bi_2Ti_2O_7$, showed cation displacement improved the thermodynamic favorability by an appreciable amount of energy (0.097 eV/Bi cation). The initial simulated annealing step outlined above is performed at the equilibrium volume identified for the ideal pyrochlore structure, but the cation displacement may be coupled to the system volume. To ensure the identification of a global minimum energy structure, we reoptimized the volume of the structure by incorporating the cation displacement. We performed the volume optimization for only the $Bi_2Ti_2O_7$ since it is the only structure that shows any significant cation displacement. We find an increase in lattice parameter from 10.23 to 10.34 Å and improved thermodynamic favorability by 0.028 eV/Bi atom. With the optimized displaced structure, the DFT lattice parameter of 10.34 Å for $Bi_2Ti_2O_7$ compares well with experimental values of ~10.36 Å. The volume increase corresponding to the asymmetric structure of the displaced $Bi_2Ti_2O_7$ is due to the steric effects of the lone pair. Similar increases in volume occur for the transition of rocksalt to litharge for PbO and SnO.[50] The total energy change from the ideal configuration to the volume optimized displaced structure for $Bi_2Ti_2O_7$ is 0.125 eV/Bi atom. This magnitude of energy change due to cation displacement in $Bi_2Ti_2O_7$ is on par with the energy change of 0.27 eV/Bi

TABLE II. The energy change and average displacement magnitudes of simple pyrochlores after simulated annealing with respect to the ideal structure is shown. (Positive value of energy corresponds to increasing thermodynamic favorability.) Systems ordered in increasing energy with the lattice constant and oxygen positional parameter are included. $Bi_2Ti_2O_7$ with volume optimized represents average values from ten different configurations.

	Energy change (eV/Bi)	Lattice constant (Å)	x (Å/Å)	Average displacements			
				Bi (Å)	B (Å)	O′ (Å)	O (Å)
$Bi_2Pt_2O_7$	9.5×10^{-4}	10.345	0.332	0.030	0.028	0.036	0.028
$Bi_2Rh_2O_7$	9.5×10^{-4}	10.190	0.332	0.048	0.033	0.034	0.034
$Bi_2Os_2O_7$	9.5×10^{-4}	10.250	0.327	0.05	0.025	0.057	0.050
$Bi_2Ru_2O_7$	0.001	10.205	0.329	0.041	0.029	0.032	0.031
$Bi_2Ir_2O_7$	0.002	10.250	0.331	0.036	0.027	0.025	0.026
$Bi_2Ti_2O_7$	0.097	10.230	0.324	0.328	0.059	0.077	0.082
Volume optimized $Bi_2Ti_2O_7$	0.146 ±0.001	10.340	0.324	0.38 ±0.02	0.07 ±0.02	0.11 ±0.01	0.10 ±0.02
$Bi_{1.87}Ru_2O_{6.903}$ [15]		10.27	0.327	0.16	0	0.01	
$Bi_2Ti_2O_7$ [16]		10.359	0.3187	0.43	0	0.15	
$Bi_{1.74}Ti_2O_{6.62}$ [17]		10.357	0.3187	0.38	0	0	

atom reported by Walsh *et al.*[50] for $Bi_2Sn_2O_7$ to change from the ideal cubic pyrochlore to the monoclinic ground state structure. We have confirmed that the bismuth pyrochlores examined in this paper retain the ideal cubic structure in agreement with all the experimental evidence. The similarity between the energy associated with cation displacement in $Bi_2Ti_2O_7$ versus a change in structure in $Bi_2Sn_2O_7$ indicates that both are feasible mechanisms for Bi-based pyrochlores to reduce the stereochemical effects of the Bi lone pair. The more complex structural change observed in $Bi_2Sn_2O_7$ is likely due to additional stereochemical effects from the Sn atom in the B site. The other bismuth pyrochlores have a different mechanism in reducing the lone pair nature of the Bi cation based on the hybridization between the Bi 6*s* and *B* cation *d* orbitals. The details of the electronic structure differences between the metal bismuth pyrochlores and $Bi_2Ti_2O_7$ are discussed in Sec. III C.

Table II also shows that although there is displacement in all six of the bismuth pyrochlores, with the exception of $Bi_2Ti_2O_7$, the average magnitude of these displacements is less than ~0.05 Å. This result agrees with available experimental observations, except for $Bi_2Ru_2O_7$, where a Bi displacement of 0.16 Å has been reported.[15] We address the differences between DFT and experiment for the $Bi_2Ru_2O_7$ system in Sec. III B 2. While the general features of the displacements that we find in $Bi_2Ti_2O_7$ are similar to experiment, there are important differences which we discuss in detail below.

1. Atomic displacement in $Bi_2Ti_2O_7$

Two experimental studies of $Bi_2Ti_2O_7$ have been reported, with their main results for the structure reproduced in Table II.[16,17] The earlier study synthesized $Bi_2Ti_2O_7$ with A_2O' network deficiency,[17] but subsequently, Hector and Wiggin[16] demonstrated that $Bi_2Ti_2O_7$ can be synthesized in stoichiometric cubic form. We will refer to these two studies as deficient and stoichiometric. Both studies analyzed the structure with x-ray and neutron powder diffraction and confirmed to be cubic pyrochlores in the $Fd\bar{3}m$ space group. The experimental work on stoichiometric $Bi_2Ti_2O_7$ reports structural details from x-ray diffraction at both room temperature and 2 K. Since our DFT calculations are at 0 K, the low temperature experimental data are used for comparison. Initial attempts to fit the diffraction data using the ideal pyrochlores structure resulted in large thermal parameters in both the stoichiometric and deficient studies, which indicates static displacements in the system.[16,17] Both studies saw the (422) reflection within the x-ray diffraction data collected, which is not possible in the ideal pyrochlore structure with isotropic atoms occupying the ideal *a*, *b*, *c*, *d*, or *f* sites of the space group and only becomes possible if the atoms are anisotropic or occupy the *e*, *g*, *h*, or *i* positions.[13] Incorporation of static displacements of Bi dramatically improved the fit to the diffraction data and reduced the thermal parameters to plausible values.[16,17] Hector and Wiggin[16] still found high O′ thermal parameters in the stoichiometric system, which were reduced by the incorporation of static displacements in a fraction of the O′ atoms. Both studies reported no significant static displacements in the B_2O_6 network. Below, we will discuss in detail the three main features of the $Bi_2Ti_2O_7$ structure (Bi cation displacement, O′ displacement, and the B_2O_6 network) and compare the two experimental studies to our DFT results.

While both experimental studies find large Bi cation displacement, they differ in the details of the resulting displaced structure. Moreover, the stoichiometric system requires the additional O′ displacement discussed above. It is important to stress that establishing the details of the static displacements experimentally is nontrivial and multiple possibilities may be indistinguishable. DFT results can assist in determin-

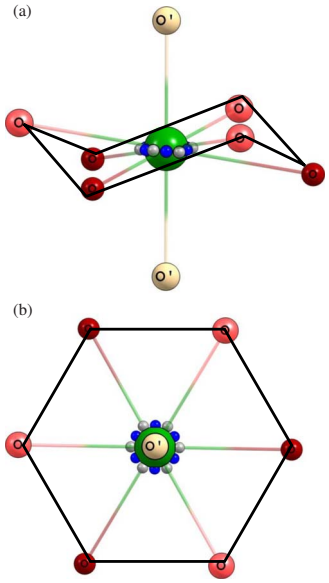

FIG. 4. (Color online) The ideal puckered ring (outlined in black) created by the six O 48*f* (dark red) atoms surrounding Bi (green) at the 16*c* site with O′ (tan) at the 8*b* site shown: (a) perpendicular to the O′-Bi-O′ chains and (b) along the O′-Bi-O′ chains. Dark red used to distinguish the O′ 48*f* atoms slightly below Bi. Small ions represent the six 96*g*(x,x,z) sites (light gray) and the six 96*h*$(y,-y,0)$ sites (dark blue) for Bi atom displacement.

ing the significance of the particular displacements reported in the experiments. A comparison between our DFT results and the experiment indicates the same general features of large Bi cation displacement and smaller displacements in the other atoms. Before we discuss the details of the Bi cation displacement it is helpful to examine the ideal local environment around the Bi cation, as shown in Fig. 4. Two views of the bonding network are shown; one perpendicular to and one along the O′-Bi-O′ chains. The Bi cation is in a scalenohedral cage with two O′ atoms and six O 48*f* atoms at the edges. The six O 48*f* atoms form a puckered ring around the Bi cation outlined in black in Fig. 4, with three slightly above and three slightly below the Bi atom.

Both experimental studies examined several different possible Bi cation displacements. The best fit to the diffraction data for the stoichiometric and deficient $Bi_2Ti_2O_7$ was Bi in the 96*g* and 96*h* crystallographic sites respectively.[16,17] There are six equivalent positions around the Bi cation for both the 96*g* site (x,x,z) and 96*h* site $(0,y,-y)$ as illustrated in Fig. 4. The assumption is that the Bi cation randomly displaces to one of these six equivalent sites, which when averaged over the bulk material results in an average ideal bulk pyrochlore structure. The 96*g* site (x,x,z) brings the Bi closer to one of the six O 48*f* atoms within the pucker ring and the displacement occurrs along the direction of the Bi-O 48*f* bond [see Fig. 4(b)], while the 96*h* site $(0,y,-y)$ involves a displacement between two of the six Bi-O 48*f* bonds. Hector and Wiggin[16] noted that the fitting quality between the 96*g* and 96*h* sites results in only a small difference and these two sites may be indistinguishable within the diffraction data. We report the details of the refined crystallographic parameters for $Bi_2Ti_2O_7$ from the two experimental studies along with our DFT results in Table III.

TABLE III. A comparison of the crystallographic parameters of $Bi_2Ti_2O_7$ obtained from two experimental studies (Refs. 16 and 17) and the results from simulated annealing at a lattice constant of 10.34 Å. The experimental temperatures differed, with + and * denoting room temperature and low temperature (≤12 K), respectively.

Atom	Site	*x*/*a*	*y*/*b*	*z*/*c*
Expt. [$Bi_2Ti_2O_7$*,[a] (10.359 Å)]				
Bi	96*g*	0.0167	0.0167	−0.0357
Ti	16*d*	1/2	1/2	1/2
O	48*f*	1/8	1/8	0.43128
O′(1)	8*a*	1/8	1/8	1/8
O′(2)	32*e*	0.215	0.215	0.215
Expt. [$Bi_{1.74}Ti_2O_{6.62}$+,[b] (10.357 Å)]				
Bi	96*h*	0	0.02745	0.97255
Ti	16*d*	1/2	1/2	1/2
O	48*f*	1/8	1/8	0.43126
O′	8*a*	1/8	1/8	1/8
This work [$Bi_2Ti_2O_7$ (10.34 Å)]				
Bi	96*h*	0	0.02418	0.97582
Bi	96*g*	0.01451	0.01451	0.96615
Bi	192*i*	0.99033	0.01934	0.02901
Ti	192*i*	0.49275	0.5	0.5
O	48*f*	1/8	1/8	0.4256
O′	192*i*	1/8	0.12984	0.13467

[a]Reference 16.
[b]Reference 17.

The main differences between Bi occupying the 96*g* and 96*h* Wyckoff sites can be seen within the altered Bi-O 48*f* and Bi-O′ bonding networks, as shown in Fig. 5. The ideal Bi-O 48*f* bonding network, as shown in Fig. 4, has six equal bond lengths. For the ideal $Bi_2Ti_2O_7$ structure determined with DFT (see Sec. III A), we found a lattice constant of 10.23 Å and an oxygen positional parameter of 0.324, which corresponds to a Bi-O 48*f* bond length of 2.55 Å. There will be four or three unique Bi-O 48*f* bond lengths if the Bi occupies the 96*g* or 96*h* site, respectively, as seen in Fig. 5(b). Here, Fig. 5(b) shows the bonding network along the O′-Bi-O′ chains for both the stoichiometric and deficient experimental structures.[16,17] Additionally, the 96*h* site displaces the Bi perpendicular to the O′-Bi-O′ chains, resulting in equal Bi-O′ bond lengths, while the 96*g* site is not directly perpendicular, resulting in two different bond lengths, as illustrated in Fig. 5(a).

Comparisons between experiment and our DFT results for displaced $Bi_2Ti_2O_7$ must be qualified due to the restricted system size in the DFT calculations. The DFT calculations are performed on one unit cell with periodic boundary conditions and therefore will not include the full set of all possible displacements sampled in a real crystal. To ensure that our conclusions about Bi cation displacement from DFT are

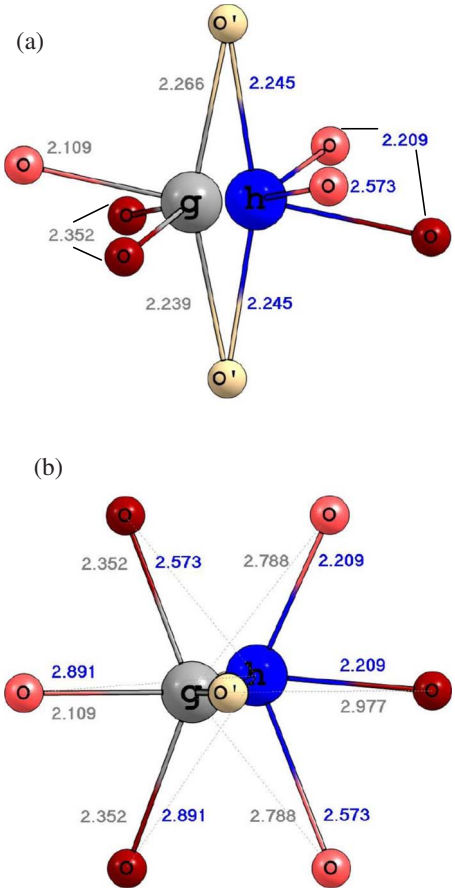

FIG. 5. (Color online) The Bi bonding networks for the two experimental studies with the six O 48*f* (red) atoms surrounding the Bi sites for the stoichiometric case at 96*g*(x,x,z) (light gray) (Ref. 16) and the deficient case at 96*h*$(y,-y,0)$ (dark blue) (Ref. 17), and O′ (tan) the at 8*b* site shown: (a) perpendicular to the O′-Bi-O′ chains and (b) along the O′-Bi-O′ chains. Only one of the six equivalent sites shown for both 96*g* and 96*h* sites along with the bond lengths in Ångstroms (light gray for the 96*g* sites and dark blue for the 96*h* sites) between these two sites and the six O 48*f* and the two O′. Dark red used to distinguish the O 48*f* atoms slightly below Bi.

valid, we performed ten distinct simulated annealing and/or relaxation runs at the optimized $Bi_2Ti_2O_7$ lattice parameter of 10.34 Å. In addition to annealing from the ideal structure with Bi at the 16*c*, site we performed similar runs on structures with small random initial displacements (−0.005–0.005 Å) on the Bi cations. Obviously, ten runs will not result in the appearance of all possible displacements, but as we discuss below, the observed displacements in our DFT calculations can be grouped into specific site types. We also modified the relaxed $Bi_2Ti_2O_7$ structures by shifting Bi atoms into other equivalent displacement sites and reoptimized the structure. Stability of such structures gives us confidence that the site types identified in our DFT calculations are fully occupied. For example, if we observe Bi relaxing to a 96*g* site, then we expect occupation of all six possible displacements into a 96*g* site in the real crystal. Differences between the energy of the ten optimized structures are negligible (less than 0.003 eV/Bi cation). The similarity in energy between our relaxed structures and the ability to identify additional equivalent displacements indicates that if a large number of simulations were performed or at a larger system size, all equivalent sites would appear with equal probability. We discuss correlation among the atomic displacements in $Bi_2Ti_2O_7$ at the end of this section.

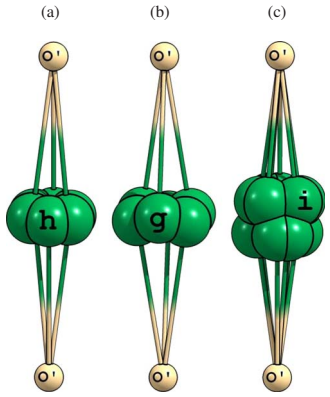

FIG. 6. (Color online) The (a) 96*h*, (b) 96*g*, and (c) 192*i* displacement sites of the Bi cations observed from simulated annealing DFT of $Bi_2Ti_2O_7$. The two O′ atoms included for orientation and all equivalent Bi displacement sites shown with one labeled.

From the ten DFT simulations, we find an average Bi cation displacement of $\sim 0.38 \pm 0.02$ Å, which is again in good agreement with the experimental values of 0.43 (0.38) Å in the stoichiometric (deficient) system (see Table II).[16,17] Within our DFT study, we find the bismuth cation displaces to both the 96*g* and 96*h* sites in addition to the 192*i* site (x,y,z) (see Table III). We determine the displacements by comparing the final relaxed positions for bismuth in each simulation with the initial ideal configuration and binned the displacement magnitudes in 0.05 Å intervals. Figure 6 illustrates each of the three sites observed in our DFT calculations for the Bi displacement, including the six equivalent 96*h* sites in Fig. 6(a), the six 96*g* sites in Fig. 6(b), and the 12 192*i* sites in Fig. 6(c).

Our DFT results present a different scenario for Bi displacement than both the stoichiometric and deficient experimental results. Both experimental studies note that the 96*g* and 96*h* sites may be indistinguishable since they overlap to a great extent. The fitting quality to the experimental diffraction data in switching between the 96*g* and 96*h* sites was reported to be minimal with a χ^2 of 4.83 and 4.86 for the 96*g* and 96*h* sites, respectively.[16] We used DFT to probe whether there is a detectable difference between the two experimental models. Beginning with the experimentally determined crystallographic structures, the energetics of the two experimental structures were examining at the experimental lattice constants using the structure optimization method detailed in Sec. II. There was no discernible difference in the energetics of the two starting structures, which further indicates that these two crystallographic sites are likely both occupied in the real $Bi_2Ti_2O_7$ crystal. To our knowledge, neither experimental study examined the possibility of multiple displacement sites. It would be worthwhile to revisit the experimental data and evaluate the fit to the diffraction data for a model incorporating the 96*g*, 96*h*, and 192*i* displacement sites, as

predicted by DFT. We suspect that the quality of the fit between the two experimental models and our DFT prediction will be indistinguishable with the diffraction data, and other more precise probes of the $Bi_2Ti_2O_7$ system will be needed to resolve this issue. Specifically, the use of infrared spectroscopy could identify any mode splitting of the Bi-O′ mode, as seen in complex bismuth-based pyrochlore.[26]

We now turn to the issue of O′ displacement, where there is also a substantial difference between the two experimental studies. The deficient structure study fixed the O′ occupation and therefore the O′ anions do not undergo any displacement. Although the isotropic thermal parameter for O′ was larger than that of the other atoms, it remained reasonable at 0.02 $Å^2$.[17] In the stoichiometric case, Hector and Wiggin[16] presented a structural model with less than 100% occupation at the ideal site. They confirmed there were no O′ deficiencies and the initial model with no O′ displacement resulted in a relatively large isotropic thermal parameter at ~0.05 $Å^2$, indicating disorder on this site.[16] Instead, they found the best fit to the diffraction data when the O′ occupied one of two sites; the ideal 8*a* site at 90% site occupancy and the 32*e* site (x,x,x) at 10% site occupancy. Displacement to the 32*e* site (x,x,x) would cause the O′ to move from its center position between four Bi cations toward two and simultaneously away from two of the Bi cations, resulting in two different bond lengths. The magnitude of the O′ displacement, for the 10% of O′ atoms that displace, determined was quite large at 0.15 Å (see Table II for details of the structure). While the displacement of only 10% of the O′ atoms in the stoichiometric system was selected based on ideal site occupation, it is difficult to find a plausible driving force for such a selective mechanism. Although we assume that they examined models with 100% displacement of O′, they did not report the quality of such models.[16] Similar to the stoichiometric system, O′ ion displacement was observed in our DFT calculations, although the average magnitude of displacement was smaller at 0.11 ± 0.01 Å, as compared to 0.15 Å (Ref. 16) and the displacement occurred at every O′ site unlike the 10% reported in the experimental study. In a single unit cell, there are eight O′ atoms, and within each of our ten simulations, the initial position was at the ideal 8b site. Within our study, every O′ ion displaces by approximately the same magnitude and in the same direction within one simulation. In our DFT relaxed structures, the displaced O′ atoms do not occupy the 32*e* site seen within the stoichiometric study. Instead, all of the displacement vectors of the O′ atoms belong to the $\langle 0.1, 0.05, 0.0 \rangle$ family, resulting in O′ occupying the 192*i* site (see Table III). To illustrate the single displacement vector of all eight O′ ions within the unit cell of one simulation, the relaxed O′ ions are shown in Fig. 7 with Bi displacement sites identified along with the 16*c* and 8*b* ideal sites. With the [110] direction indicated in Fig. 7, it can be seen that the O′ displaced ions follow the same vector within one unit cell and there appears to be a relationship between the O′ and Bi displacements further discussed below. This O′ directional displacement is consistent with other complex bismuth-based pyrochlores refinement, but in those systems, the O′ displacement is along the [110] direction.[13] The occurrence of O′ anion displacement coincides with Bi cation displacement in $Bi_2Sn_2O_7$,[51] $Bi_2Ru_2O_7$,[15] and $Bi_2Ti_2O_7$.[16]

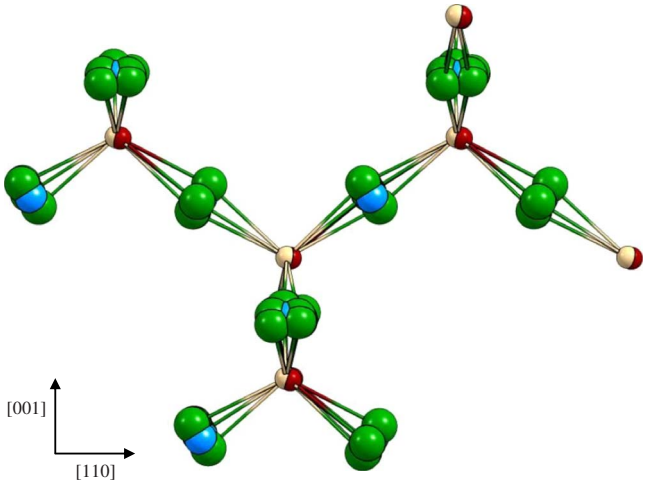

FIG. 7. (Color online) The Bi-O′ bonding network with the 8*a* site (tan), the displaced O′ (dark red), the 16c site (light blue), and the 96*g*, 96*h*, and 192*i* Bi displacement sites (dark green), determined in all ten simulated annealings. The bonding network direction provided indicates the displaced sites appear correlated along the [110] direction, with an alternating of the orientation with respect to the ideal site, either in front or behind.

The difference in nature and magnitude of O′ displacement between these structures depends on the B_2O_6 network. Even though the O′ displacement within this work differs from the experimental works for simple bismuth pyrochlores, the identification follows the coupling of O′ displacement and Bi cation displacement.

We conclude the discussion on the structure of $Bi_2Ti_2O_7$ with the B_2O_6 network. In both experimental studies, the oxygen at the 48*f* site was unaffected and both determined an oxygen positional parameter of 0.3187. Since there was no change in the oxygen positional parameter and Ti atoms were at the 16*d* site in the experimental models, the Ti-O 48*f* bonding remained completely unaffected by the Bi cation displacement. By contrast, within our study, the Ti atoms showed displacement with an average of 0.07 ± 0.02 Å, but did not have a significant effect on the average Ti-O 48*f* bond length found at 1.965 Å, matching both experimental studies. Although the average bond length found in our study was unaffected by displacement, the distribution of Ti-O 48*f* bond lengths observed within each TiO_6 octahedron ranged from 1.88 to 2.07 Å, with the average in each octahedron equal to 1.965 Å. The small average magnitude of the Ti displacement seen in our study may indicate that these displacements could be absorbed by the thermal parameters experimentally and without direct probing may be overlooked.

Based on the observations made within this study, reexamination of the experimental structural parameters with emphasis paid on the site(s) of Bi and any potential displacement of the Ti cations could provide further insight into this system. Since our study identified multiple Wyckoff sites occupied by displaced Bi cations, it would be beneficial to determine if this is also observed within the experimental crystal and if there is any short-range ordering of displacement sites. Our DFT results indicate that the multiple displacement positions around the ideal Bi site are energetically

equivalent, but we have not calculated the barriers to hop among these displacement sites. This hopping mechanism was proposed in bismuth-based pyrochlores by Nino *et al.*,[52] Levin *et al.*,[13] Vanderah *et al.*[12] and Somphon *et al.*[53] for other pyrochlore compounds, exhibiting cation displacement. Future DFT studies probing the potential energy surface of bismuth cation hopping between these displacement sites will assist our understanding of the dielectric properties of these materials.

Up to this point, we have concentrated on the structure of $Bi_2Ti_2O_7$ in terms of an average structure where we assume that the displacements discussed randomly occur but with equal probability. The experimental studies could not probe any correlation within the atom displacements in $Bi_2Ti_2O_7$ since they only have information on the average structure. Bismuth-based pyrochlores have recently been studied as "spin-ice" pyrochlores, where the tetrahedral bonding of O′ ions around the central Bi cation are compared to the ice equivalent of oxygen-centered tetrahedrons with two hydrogen ions covalently bonded at a smaller length and two more distantly bonded by hydrogen bonding.[14] Structural analysis of these complex pyrochlores has shown short-range order.[10] Such characteristics are mirrored within our observed displacements of bismuth in $Bi_2Ti_2O_7$. Both the Bi displacement and O′ displacement seen within our study follow the "two-long, two-short" bonds, resulting in each tetrahedron of Bi_4O' comprised of, on average, two bonds at 2.2 Å and two bonds at 2.3 Å. A relationship between the Bi displacement sites can be seen in Fig. 7 with the displacement site alternating between in front of or behind the ideal 16*c* site along the [110] direction. We find that within any given simulation, these two alternating sites belong to two of the three Wyckoff sites we have identified for Bi displacement (i.e., 96*g*, 96*h*, and 192*i*), occurring in pairs of either (96*g* and 96*h*) or (96*g* and 192*i*) sites. We stress that for no individual simulations of a unit cell, do we observe all three Bi displacements, indicating that there is a strong correlation between the Bi cation displacements.

Previous studies have investigated the displacement within bismuth-based pyrochlores to identify any correlation with results depending on the cation(s) occupying the *B* site.[14] In the case of Bi_2InNbO_7, the observation of diffuse streaking at particular Bragg reflections in electron diffraction patterns indicates the occurrence of β-cristobalite-type displacive disorder in the Bi_2O' substructure.[53] In this structure along with $Bi_{1.89}Fe_{1.16}Nb_{0.95}O_{6.95}$, displacement within the Bi_4O' tetrahedron network is highly correlated and believed to be related to the dielectric properties.[10,52,54,55] Similar correlation between Bi displacements are observed within our study of $Bi_2Ti_2O_7$ (Fig. 7) and within the electronic structure detailed in Sec. III C. Although electron diffraction patterns from experimental studies of this system are not known, it would be of interest to investigate the presence of similar indicators of displacive disorder within such patterns.

2. *Atomic displacement in* $Bi_2Ru_2O_7$

Experimentally, $Bi_2Ti_2O_7$ is not the only simple bismuth pyrochlore that exhibits Bi cation displacement. Avdeev *et al.*[15] report a bismuth displacement of 0.16 Å in $Bi_2Ru_2O_{7-\delta}$. In their investigation, it is determined that Bi occupies the 96*h* site and O′ occupies the 32*e* site. The displacement of the O′ ions is relatively small at 0.01 Å. However, despite multiple attempts with simulated annealing including at various volumes, we did not observe any substantial bismuth displacements for the $Bi_2Ru_2O_7$ system. The energetics and magnitude of cation displacement are both negligible in our investigation, with only 0.006 eV/Bi cation associated with an average Bi displacement of only 0.05 Å. Similar to $Bi_2Ti_2O_7$, we performed calculations on the experimentally reported displaced structure, with the experimental structure found to be less stable by 1.8 eV/Bi cation when compared to the ideal undisplaced structure that we report in Sec. III A. When compared to the energy change in the titante system, the magnitude indicates that the experimental structure is highly unfavorable. Since the lattice constant may be coupled to the Bi displacement, we varied the volume within the experimental structure, but it remains less favorable than the ideal undisplaced system by 1.7 eV/Bi. Recently, Goodwin *et al.*[56] examined the defective $Bi_2Ru_2O_{7-\delta}$ using diffuse electron diffraction. They found that a structural model involving beta-cristobalite-type displacement for Bi cations best fitted the diffraction features. We have also performed DFT calculations using the structural model of Goodwin *et al.*,[56] and again we find that the cation displacement is not favored. Cation displacement was again not favorable with the consideration of spin polarization for both the simulated annealing of the ideal configuration and in the atomic relaxation of the experimental structure.

Between the simulated annealing runs performed on both the ideal starting structure and the experimentally determined displaced structure, our DFT results suggest that cation displacement is not critical to stabilize the $Bi_2Ru_2O_7$ system. As we show in the next section, based on the electronic structure of the metallic bismuth pyrochlores, there is no indication that $Bi_2Ru_2O_7$ should dramatically behave different from the other metallic bismuth pyrochlores. The source of the discrepancies between DFT and the recent experimental studies is not currently clear. The $Bi_2Ru_2O_{7-\delta}$ in the experiments is defective in O′ and Bi, possible triggering the observed bismuth cation displacement, but we have not probed the role of O′ vacancies on the structure of the bismuth pyrochlores. Both experimental studies assumed that the vacancies do not play a significant role in the observed cation displacements. Goodwin *et al.*[56] found a good fit to the diffraction patterns without the O′ vacancies, which gives support to this assumption. Future DFT and experimental studies are needed to clarify the role of O′ vacancies and may assist in resolving the conflict between DFT and experimental results. To our knowledge, there is no experimental study of stoichiometric $Bi_2Ru_2O_7$.

C. Electronic structure

To shed light on our observation of large cation displacements solely in the $Bi_2Ti_2O_7$ system, we examined the electronic structure of the simple bismuth pyrochlores and the displaced $Bi_2Ti_2O_7$. Structure distortions in Bi and Pb based oxides are quite common[30,50] and are usually attributed to the sterochemical activity of the lone pair on the cation. Re-

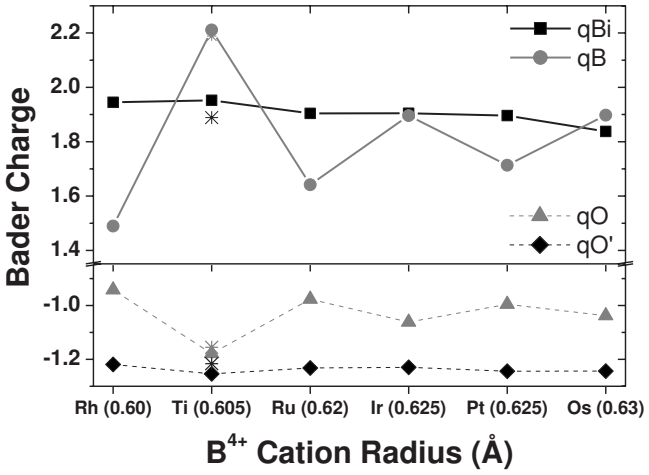

FIG. 8. Bader atomic charges in units of e for the Bi, B, O $48f$ and O′ ion presented for each of the bismuth pyrochlores. The charges within the Bi_2O' network are darker, while the charges associated with the B_2O_6 network are lighter colored. The lines are drawn as a visual aid, solid for the cations, and dashed for the oxygen ions. The averaged Bader charges for the $Bi_2Ti_2O_7$ displaced system at 10.34 Å are indicated by the stars.

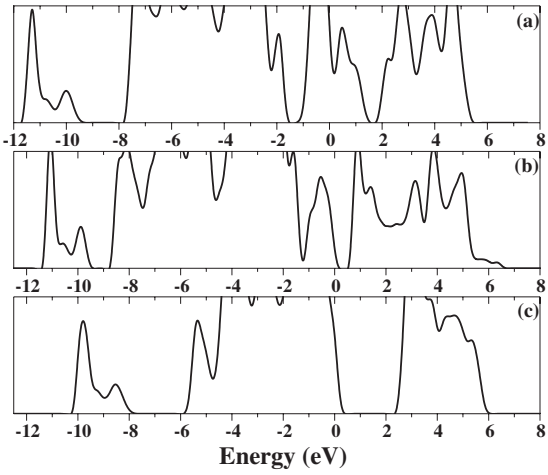

FIG. 9. Density of states in arbitrary units for (a) $Bi_2Ru_2O_7$, (b) $Bi_2Pt_2O_7$, and (c) $Bi_2Ti_2O_7$ in the ideal cubic pyrochlores structure with no cation displacement. The zero energy value represents the Fermi level.

cently, electronic structure calculations of SnO, PbO, and Bi_2O_3 oxides have shown that the classical picture of lone pair formation due to the hybridization of s and p orbitals of the metal cation is not correct.[50,57,58] Instead, they found that the asymmetric electronic structure in these materials is due to interactions between the metal cation s and p and O $2p$ states, and it is these interactions that stabilize the distorted structure.[50,57,58] The Bi pyrochlores are more complex since there are two cations and the above understanding in the oxides does not directly shed light on why only the $Bi_2Ti_2O_7$ shows appreciable distortions. Below, we discuss the electronic structure obtained from our DFT results using Bader atomic charges, total and partial electronic density of states (DOS and pDOS), and the electron localization function (ELF) for each of the bismuth-based pyrochlores. We find that the atomic displacements in $Bi_2Ti_2O_7$ are favored due to the Bi s and p orbitals interactions with the O′ p orbital in a manner similar to that reported by Walsh and co-workers[50,57,59] for distorted PbO, SnO, and $Bi_2Sn_2O_7$. The metallic bismuth pyrochlores do not show displacement due to weaker Bi-O′ interactions combined with stronger Bi-O interactions at the Fermi level. These differences in bonding between Bi-O′ are sufficient to suppress the formation of the lone pair upon cation displacement and therefore large cation displacement is not favored in the metallic bismuth pyrochlores. An examination of the ELF of the distorted $Bi_2Ti_2O_7$ with Bi cation displacement clearly displays the asymmetric electronic distribution around the Bi cation indicative of a lone pair and alters the bonding network.

The distribution of charges within the system of the ions aids in characterizing the bonding between atoms. We have determined the atomic charges based on the Bader criteria for decomposing the electron density[60] using the code of Henkelman *et al.*[61] Figure 8 presents the Bader charges for all the Bi pyrochlores in this study plotted against the B cation radius. The values for the various ions are comparable to values seen in a recent DFT investigation of La- and Y-based pyrochlores.[42] We have examined the trends of the Bader charges versus the cation radius, but similar to the bond lengths (see Sec. III A), we did not find any simple trend. The deviation between the atomic Bader charges and the formal ionic charge indicates the degree of covalency. All ions deviate from their formal charge values, indicating the importance of covalency in these systems. The smallest difference between the DFT atomic charge and the formal charge is found in the $Bi_2Ti_2O_7$ system, indicating that the Ti-O bond is less covalent than the B-O bond in the metallic pyrochlores. The degree of covalency of the cation-O bonds in bismuth pyrochlores was previously explored using electronegativity values of the ions.[62] The larger the difference in electronegativity between the two bonded atoms, the more ionic the bond. Based on this relationship, Wang *et al.*[62] determined that the B-O bond should be least covalent in $Bi_2Ti_2O_7$, which matches the conclusion from the DFT atomic charges. Therefore, in systems that do not show large cation displacements, the B-O bonds are more covalent. Figure 8 also indicates the change in atomic charges in $Bi_2Ti_2O_7$ due to atomic displacement. We do not see dramatic changes in the charge values, but Bi and O′ atoms undergo the greatest change due to increased Bi-O′ interaction after displacement.

The DOS of each system was examined to identify electronic structure characteristics. Figure 9 presents the DOS for some of the bismuth pyrochlores without cation displacement. The known metallic bismuth pyrochlores of $Bi_2Ru_2O_7$, $Bi_2Ir_2O_7$, $Bi_2Rh_2O_7$, and $Bi_2Os_2O_7$ all have qualitatively similar DOS that indicate metallic behavior; therefore, Fig. 9(a) shows only the $Bi_2Ru_2O_7$ DOS. As seen in Fig. 9(b), the DOS for $Bi_2Pt_2O_7$ is slightly different from the other transition metal bismuth pyrochlores and shows a small band gap of 0.5 eV. Experimental work identified $Bi_2Pt_2O_7$ as a semimetal[9] but did not provide information on the band gap. It is experimentally known that $Bi_2Ti_2O_7$ behaves as an in-

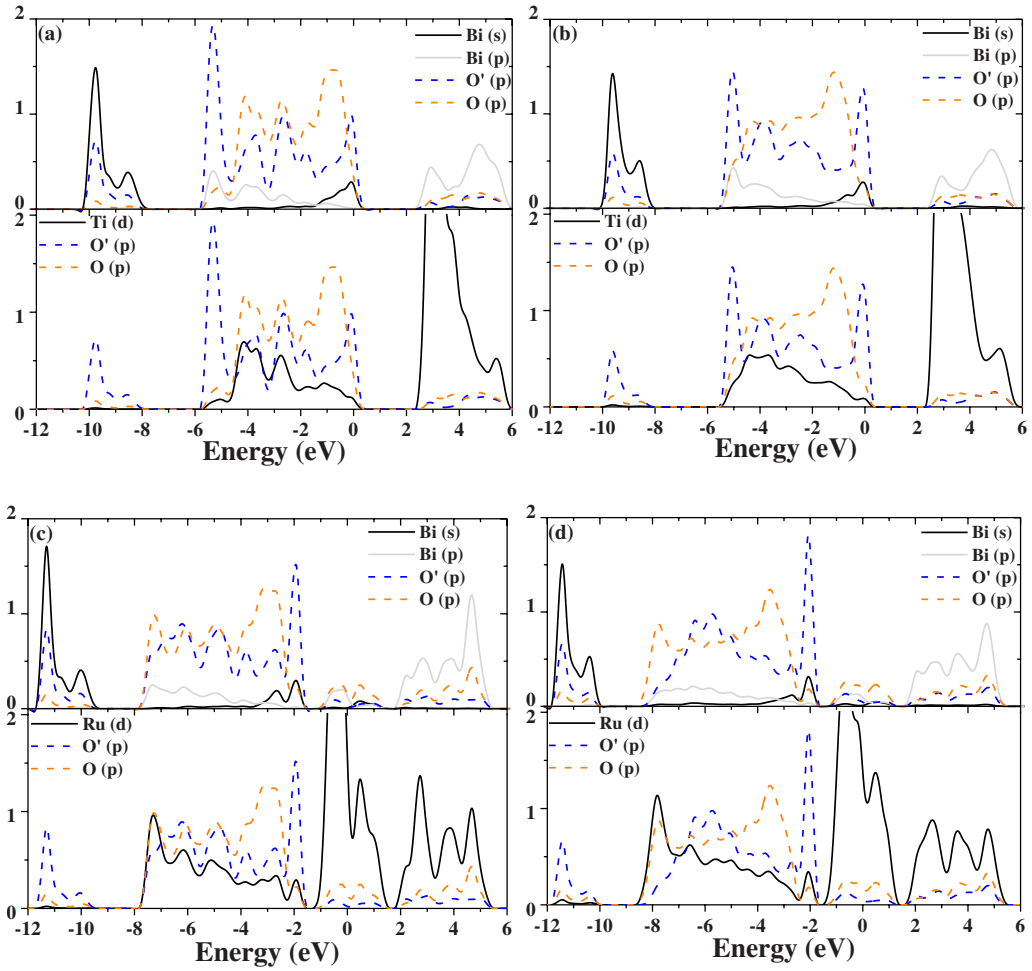

FIG. 10. (Color online): Partial density of states in arbitrary units of Bi (6*s*), Bi (6*p*) and B (*d*) for the $Bi_2Ti_2O_7$ pyrochlore (a) before and (b) after displacement and volume optimization and the $Bi_2Ru_2O_7$ pyrochlore (c) undistorted and (d) with forced displacement.

sulator and Fig. 9(c) shows our DFT results predict a band gap of 1.8 eV compared to the value of 2.95 estimated from UV-Vis adsorption spectrum by Yao *et al.*[63] In general, DFT is known to underestimate band gaps, and the value determined here is comparable to a value of 2 eV determined by Seshadri[14] from linear muffin-tin orbital calculations.

The pDOS is shown for undistorted and distorted $Bi_2Ti_2O_7$ and $Bi_2Ru_2O_7$ in Fig. 10. Again, we show only the $Bi_2Ru_2O_7$ pDOS, but the other metallic bismuth pyrochlores have essentially the same features. We qualitatively find similar mixing of states to prior DFT studies of $Bi_2Ru_2O_7$ and undistorted $Bi_2Ti_2O_7$.[14,15] The Bi 6*s* and 6*p*, B cation *d*, and the O 2*p* states appear in the conduction and valence bands. We initially focus our discussion on the main features that impact the observed cation displacement in $Bi_2Ti_2O_7$. A comparison of the pDOS of undistorted $Bi_2Ti_2O_7$, with recently reported studies of PbO, SnO, and $Bi_2Sn_2O_7$,[30,50,57] shows several sharp similarities. Bi *s* states show mixing with O′ *p* states in the lower part of the valence band (−10 to −8 eV) and near the Fermi level at the top of the valence band. The Bi *s*-O′ *p* mixing near the Fermi level observed in undistorted $Bi_2Ti_2O_7$ [Fig. 10(a)] was reported in PbO, SnO, and $Bi_2Sn_2O_7$ and was associated with antibonding interactions.[30,50,57] There is mixing between Bi *p* states with O′ *p* states in the top region of the valence band, which is further enhanced in the $Bi_2Ti_2O_7$ after cation displacement and volume optimization [see Figs. 10(a) and 10(b)]. The Bi *s*-O′ *p* mixing near the Fermi level is also enhanced by cation displacement. A recent study by Walsh and Watson[59] on the distorted α phase and undistorted cubic γ phase of $Bi_2Sn_2O_7$ showed similar differences in the Bi-O′ interactions as our undistorted and distorted $Bi_2Ti_2O_7$ pDOSs. The Bi *p*-(Bi *s*-O′ *p*) interactions are associated with the asymmetric electron density of the lone pair and is the same mechanism observed in several other oxides that distort due to the presence of a lone pair.[59,30,50,57] Other oxides, such as PbO and SnO, do show a larger change in the degree of the mixing of Bi cation-O upon a change from high to low symmetry structures. Therefore, the formation of the lone pair is not due to direct Bi *s*-Bi *p* hybridization but instead is a result of Bi *s* and *p* hybridization with O′ *p* states. There are interactions between Bi and O *p* states in $Bi_2Ti_2O_7$, but the Bi *s*-O *p* interactions are less pronounced than the Bi *s*-O′ *p* interactions and occur at an energy further down from the Fermi level.

As seen in a comparison of Figs. 10(a) and 10(c), there are many differences between the pDOS of the undistorted $Bi_2Ti_2O_7$ and the metallic bismuth pyrochlores ($Bi_2Ru_2O_7$).

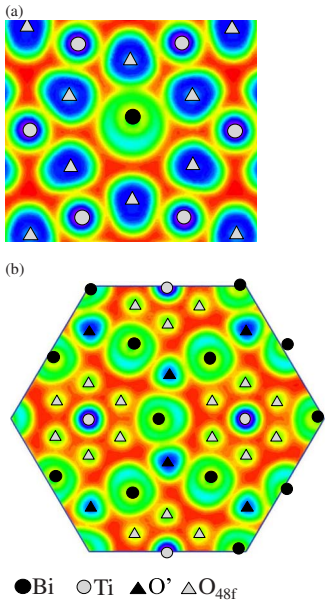

FIG. 11. (Color online) The electron localization of the displaced $Bi_2Ti_2O_7$ at 10.34 Å for the (a) (111) plane with Bi in the center and the (b) $(\bar{1}11)$ plane with the Bi, Ti, O′, and O 48*f* ions indicated. The ELF values range from 0 (light red) to 1 (dark purple).

$Bi_2Ru_2O_7$ shows more overlap between Ru *d* and O *p* states over a broader range than found between Ti *d* and O *p* in $Bi_2Ti_2O_7$, which reinforces the conclusion from the Bader atomic charges that the *B*-O bond is more covalent in the metallic pyrochlores. The Bi *s*-O′ *p* mixing in $Bi_2Ru_2O_7$ is similar to $Bi_2Ti_2O_7$ for the lower energy region in the valence band, but the Bi *s* and *p* mixing with O′ *p* states at the top of the valence band shows several differences. First, the Bi *s*-O′ *p* interactions in $Bi_2Ru_2O_7$, similar to the antibonding interactions found in $Bi_2Ti_2O_7$, occur 2 eV below the Fermi level. There is also mixing between the Bi *s* and *p* states with O 48*f* across the Fermi level along with some mixing of the Bi *s* and O′ *p* states. In general, there is more mixing between the Bi states and O 48*f* *p* states in $Bi_2Ti_2O_7$, and while additional mixing of the Bi *s* and O′ *p* states is observed at the Fermi level, it is much less pronounced than the Bi-O 48*f* interactions. The net effect of the greater mixing of Ru *d* and O 48*f* *p* states on the top of the valence band is a reduction of the Bi-O′ interactions. This reduction is sufficient to eliminate the interactions that favor lone pair formation upon cation displacement in $Bi_2Ru_2O_7$. We have examined the pDOS for a displaced $Bi_2Ru_2O_7$, as shown in Fig. 10(d), and do not find as large an enhancement of Bi-O′ mixing that occurs in displaced $Bi_2Ti_2O_7$.

The ELF for the $Bi_2Ti_2O_7$ displaced system on the (111) and $(\bar{1}11)$ plane is shown in Figs. 11(a) and 11(b), respectively. Figure 11(a) provides details of the Bi-O 48*f* environment, while Fig. 11(b) highlights the interaction between the Bi-O′ network and the Ti-O 48*f* network. Within Fig. 11(a), the Bi cation strongly bonds to three of the six O 48*f* anions, leaving a small space between the remaining three O 48*f* anions and the Bi cation. A more strongly localized lobe of electron density, corresponding to the lone pair, partially occupies the space. Figure 11(a) indicates that the Bi cation displacement allows the lone pair on the Bi cation to occupy space that would be otherwise unavailable within the ideal configuration. A similar ELF structure has been observed for the bismuth-based $SrBi_2Ta_2O_9$ by Seshadri,[14] where the electrons preferentially localize to one half of the ion. Figure 11(b) illustrates the correlation with the Bi cation displacements explained in Sec. III B 1, with the Bi displacement simultaneously alternating toward and away from the Ti-O 48*f* networks. As mentioned in Sec. III B 1, Somphon *et al.*[53] observed this correlated Bi displacement within the more complex Bi_2InNbO_7 and Bi_2FeNbO_7 compounds and indicated that it would affect the displacive disorder and therefore the dielectric properties. We have examined the ELF for distorted $Bi_2Ru_2O_7$ (not shown) and observe no lone pair formation, which reinforces the conclusion from the pDOS that atomic displacement is not favored in $Bi_2Ru_2O_7$.

IV. SUMMARY

By using DFT calculations, we examined a range of cubic $Bi_2B_2O_6O'$ (*B*=Ti, Ru, Rh, Ir, Os, and Pt) pyrochlores and report the structural parameters along with the electronic structure of the bismuth pyrochlores in their ideal cubic, defect-free structure. The role of cation displacements within the cubic structure was investigated, with the identification of atomic displacement in the $Bi_2Ti_2O_7$ compound. The atomic displacement stabilizes this structure with an energy change of similar magnitude to that of other bismuth-based pyrochlores. In $Bi_2Ti_2O_7$, we found an average displacement of 0.38 Å for the Bi cation, 0.07 Å for the Ti cation, 0.11 Å for the O′ anion, and an energy change of ~0.15 eV/Bi atom. The Bi cation displacements appear to be correlated as seen in other more complex bismuth pyrochlores. Examination of the electronic structure shows that the main difference between $Bi_2Ti_2O_7$ and the metallic bismuth pyrochlores is the extent of Bi-O′ interactions. In $Bi_2Ti_2O_7$, we observe more overlap of Bi *s* and *p* states with O 2*p* states similar to the reported electronic structure of $Bi_2Sn_2O_7$, PbO, and SnO,[50,57] which leads to the asymmetric electronic structure around the Bi cation and the displacement of cations in $Bi_2Ti_2O_7$. Our DFT results match the general understanding from experimental studies but underestimate the displacement in $Bi_2Ru_2O_7$ compared to experimental results of defective $Bi_2Ru_2O_{7-\delta}$.[15] Further work in examining the role of vacancies may assist in resolving the differences between our DFT results and experimental work on $Bi_2Ru_2O_7$.

ACKNOWLEDGMENTS

We thank Lu Cai for assistance in the drawing of Fig. 1. We also thank Simon Phillpot and Susan Sinnott for helpful discussions. We acknowledge the University of Florida High-Performance Computing Center (http://hpc.ufl.edu) for providing computational resources. One of the authors (J.C.N.) would like to acknowledge the financial support for this work by the U.S. National Science Foundation (CAREER Grant No. DMR-0449710).

*Corresponding author; aasthagwi@che.ufl.edu

[1] D. P. Cann, C. A. Randall, and T. R. Shrout, Solid State Commun. **100**, 529 (1996).
[2] B. J. Wuensch, K. W. Eberman, C. Heremans, E. M. Ku, P. Onnerud, E. M. E. Yeo, S. M. Haile, J. K. Stalick, and J. D. Jorgensen, Solid State Ionics **129**, 111 (2000).
[3] R. C. Ewing, W. J. Weber, and J. Lian, J. Appl. Phys. **95**, 5949 (2004).
[4] A. Cleave, R. W. Grimes, and K. Sickafus, Philos. Mag. **85**, 967 (2005).
[5] B. J. Kennedy, J. Solid State Chem. **123**, 14 (1996).
[6] R. C. Vassen, X. Tietz, T. Basu, and D. Stöver, J. Am. Ceram. Soc. **83**, 2023 (2000).
[7] G. Suresh, G. Seenivasan, M. V. Krishnaiah, and P. Srirama Murti, J. Nucl. Mater. **249**, 259 (1997).
[8] P. K. Schelling, S. R. Phillpot, and R. W. Grimes, Philos. Mag. Lett. **84**, 127 (2004).
[9] M. A. Subramanian, G. Aravamudan, and G. V. Subba Rao, Prog. Solid State Chem. **15**, 55 (1983).
[10] R. L. Withers, T. R. Welberry, A. K. Larsson, Y. Liu, L. Noren, H. Rundlof, and F. J. Brink, J. Solid State Chem. **177**, 231 (2004).
[11] J. C. Nino, in *Materials Science and Engineering* (The Pennsylvania State University, University Park, PA, 2002).
[12] T. A. Vanderah, I. Levin, and M. W. Lufaso, Eur. J. Inorg. Chem. **2005**, 2895 (2005).
[13] I. Levin, T. G. Amos, J. C. Nino, T. A. Vanderah, C. A. Randall, and M. T. Lanagan, J. Solid State Chem. **168**, 69 (2002).
[14] R. Seshadri, Solid State Sci. **8**, 259 (2006).
[15] M. Avdeev, M. K. Haas, J. D. Jorgensen, and R. J. Cava, J. Solid State Chem. **169**, 24 (2002).
[16] A. L. Hector and S. B. Wiggin, J. Solid State Chem. **177**, 139 (2004).
[17] I. Radosavljevic, J. S. O. Evans, and A. W. Sleight, J. Solid State Chem. **136**, 63 (1998).
[18] B. Melot, E. Rodriguez, T. Proffen, M. A. Hayward, and R. Seshadri, Mater. Res. Bull. **41**, 961 (2006).
[19] R. D. Shannon, Mater. Res. Bull. **32**, 751 (1976).
[20] J. C. Nino, H. J. Youn, M. T. Lanagan, and C. A. Randall, J. Mater. Res. **17**, 1178 (2002).
[21] J. Nino, M. T. Lanagan, and C. A. Randall, J. Appl. Phys. **89**, 4512 (2001).
[22] J. C. Nino, M. T. Lanagan, and C. A. Randall, J. Mater. Res. **16**, 1460 (2001).
[23] I. Levin, T. G. Amos, J. C. Nino, T. A. Vanderah, I. M. Reaney, C. A. Randall, and M. T. Lanagan, J. Mater. Res. **17**, 1406 (2002).
[24] J. C. Nino, I. M. Reaney, M. T. Lanagan, and C. A. Randall, Mater. Lett. **57**, 414 (2002).
[25] Y. Liu, R. L. Withers, T. R. Welberry, H. Wang, and H. L. Du, J. Solid State Chem. **179**, 2141 (2006).
[26] M. H. Chen, D. B. Tanner, and J. C. Nino, Phys. Rev. B **72**, 054303 (2005).
[27] L. W. Fu, H. Wang, S. X. Shang, X. L. Wang, and P. M. Xu, J. Cryst. Growth **139**, 319 (1994).
[28] S. P. Yordanov, I. Ivanov, and C. P. Carapanov, J. Phys. D **31**, 800 (1998).
[29] X. N. Yang, B. B. Huang, H. B. Wang, S. X. Shang, W. F. Yao, and J. Y. Wei, J. Cryst. Growth **270**, 98 (2004).
[30] A. Walsh, G. W. Watson, D. J. Payne, G. Atkinson, and R. G. Egdell, J. Mater. Chem. **16**, 3452 (2006).
[31] B. J. Kennedy, Mater. Res. Bull. **32**, 479 (1997).
[32] B. J. Kennedy, Physica B **241-243**, 303 (1997).
[33] G. Kresse and J. Furthmuller, Comput. Mater. Sci. **6**, 15 (1996).
[34] G. Kresse and J. Furthmüller, Phys. Rev. B **54**, 11169 (1996).
[35] G. Kresse and J. Hafner, Phys. Rev. B **47**, 558 (1993).
[36] G. Kresse and J. Hafner, Phys. Rev. B **49**, 14251 (1994).
[37] P. E. Blöchl, Phys. Rev. B **50**, 17953 (1994).
[38] G. Kresse and D. Joubert, Phys. Rev. B **59**, 1758 (1999).
[39] W. Kohn and L. J. Sham, Phys. Rev. **140**, A1133 (1965).
[40] Z. G. Wu, R. E. Cohen, and D. J. Singh, Phys. Rev. B **70**, 104112 (2004).
[41] Z. G. Wu and R. E. Cohen, Phys. Rev. B **73**, 235116 (2006).
[42] J. M. Pruneda and E. Artacho, Phys. Rev. B **72**, 085107 (2005).
[43] J. P. Perdew, K. Burke, and M. Ernzerhof, Phys. Rev. Lett. **77**, 3865 (1996).
[44] M. Methfessel and A. T. Paxton, Phys. Rev. B **40**, 3616 (1989).
[45] H. J. Monkhorst and J. D. Pack, Phys. Rev. B **13**, 5188 (1976).
[46] R. A. McCauley, J. Appl. Phys. **51**, 290 (1980).
[47] L. Minervini, R. W. Grimes, Y. Tabira, R. L. Withers, and K. E. Sickafus, Philos. Mag. A **82**, 123 (2002).
[48] M. Pirzada, R. W. Grimes, L. Minervini, J. F. Maguire, and K. E. Sickafus, Solid State Ionics **140**, 201 (2001).
[49] W. W. Barker, J. Graham, O. Knop, and F. Brisse, in *The Chemistry of Extended Defects in Non-Metallic Solids*, edited by L. Eyring, and O'Keeffe (North Holland, London, 1970), p. 198.
[50] A. Walsh and G. W. Watson, J. Solid State Chem. **178**, 1422 (2005).
[51] I. R. Evans, J. A. K. Howard, and J. S. O. Evans, J. Mater. Chem. **13**, 2098 (2003).
[52] J. C. Nino, M. T. Lanagan, and C. A. Randall, J. Appl. Phys. **89**, 4512 (2001).
[53] W. Somphon, V. Ting, Y. Liu, R. L. Withers, Q. Zhou, and B. J. Kennedy, J. Solid State Chem. **179**, 2495 (2006).
[54] S. Kamba, V. Porokhonskyy, A. Pashkin, V. Bovtun, J. Petzelt, J. C. Nino, S. Trolier-McKinstry, M. T. Lanagan, and C. A. Randall, Phys. Rev. B **66**, 054106 (2002).
[55] C. Ang, Z. Yu, H. J. Youn, C. A. Randall, A. S. Bhalla, L. E. Cross, J. Nino, and M. Lanagan, Appl. Phys. Lett. **80**, 4807 (2002).
[56] A. L. Goodwin, R. L. Withers, and H. B. Nguyen, J. Phys.: Condens. Matter **19**, 335216 (2007).
[57] A. Walsh and G. W. Watson, Phys. Rev. B **70**, 235114 (2004).
[58] A. Walsh, G. W. Watson, D. J. Payne, R. G. Edgell, J. H. Guo, P. A. Glans, T. Learmonth, and K. E. Smith, Phys. Rev. B **73**, 235104 (2006).
[59] A. Walsh and G. W. Watson, Chem. Mater. **19**, 5158 (2007).
[60] R. Bader, *Atoms in Molecules: A Quantum Theory* (Oxford University Press, New York, 1990).
[61] G. Henkelman, A. Arnaldsson, and H. Jonsson, Comput. Mater. Sci. **36**, 354 (2006).
[62] X. L. Wang, H. Wang, and X. Yao, J. Am. Chem. Soc. **80**, 2745 (1997).
[63] W. F. Yao, H. Wang, X. H. Xu, J. T. Zhou, X. N. Yang, Y. Zhang, and S. X. Shang, Appl. Catal., A **259**, 29 (2004).